# Numerical and Theoretical Studies of Turbulence and Transport with E × B Shear Flows

Z. Lin, M. S. Chance, T. S. Hahm, J. A. Krommes, W. W. Lee, I. Manuilskiy,
H. E. Mynick, H. Qin, G. Rewoldt, W. M. Tang, and R. B. White
*Princeton Plasma Physics Laboratory, Princeton University, Princeton, NJ 08543*

(3/29/1999)
D2,Tt

## Abstract

This paper reports: (1) substantial transport reduction by turbulence-driven $\mathbf{E} \times \mathbf{B}$ flows observed in 3D nonlinear gyrokinetic simulations of microturbulence in magnetically-confined toroidal plasmas; (2) analytical derivation of the effective shearing rate for the time-dependent $\mathbf{E} \times \mathbf{B}$ flow; (3) interpretation of experimental data using linear gyrokinetic microinstability rotation models of $\mathbf{E} \times \mathbf{B}$ shear; and (4) other developments in gyrokinetic theory and simulation.

## I. INTRODUCTION

There is accumulating evidence that $\mathbf{E} \times \mathbf{B}$ flow shear suppression of turbulence is the most likely mechanism responsible for various forms of confinement enhancement in magnetically-confined plasmas. Understanding the mechanisms of turbulence suppression and discovering techniques to control turbulence are needed for developing magnetic fusion. Recent experimental data [1] from tokamaks core region revealed the presence of small radial scale $\mathbf{E} \times \mathbf{B}$ flows that cannot be explained by the existing neoclassical theory. These observations point to the possibility that $\mathbf{E} \times \mathbf{B}$ flows generate spontaneously and regulate the turbulence. Turbulent transport is believed to arise from electrostatic pressure-gradient driven instabilities. These highly complex nonlinear phenomena can be effectively investigated by numerical experiments. One of the most promising approaches is gyrokinetic particle simulation. Our gyrokinetic simulations [2] observed substantial reduction of heat transport due to the turbulence-generated $\mathbf{E} \times \mathbf{B}$ flows. These simulations of ion-temperature-gradient turbulence retained gyrokinetic ion dynamics and assumed adiabatic electron response. We have also found that zonal flow structure plays a crucial role in causing the outstanding differences between global and local simulation results. The effective shearing rate for time-dependent $\mathbf{E} \times \mathbf{B}$ flow is derived [3]. It is shown that the high frequency components of zonal flows are not effective in reducing turbulence. Finally, an improved rotation model for linear microinstability calculations is described and applications to experimental data are presented [4].

## II. GYROKINETIC SIMULATIONS OF TURBULENCE-DRIVEN E × B FLOWS

We have developed a fully three-dimensional global gyrokinetic toroidal code (GTC) [2] for studying both turbulence and neoclassical physics [5]. The code uses a general geometry Poisson solver and Hamiltonian guiding center equations of motion in magnetic coordinates to treat both advanced axisymmetric and nonaxisymmetric configurations using realistic

numerical MHD equilibria. This global code takes into account equilibrium profile variation effects has low particle noise. Using a non-spectral Poisson solver [6], the equilibrium quantities such as gyroradius and sound speed are allowed to be spatially dependent. In the simulations reported here, these equilibrium parameters are assumed to be uniform based on a two-scale expansion. Furthermore, a single code can simulate both a full poloidal cross section and an annular box to provide a connection between global and local simulations. The GTC code was implemented as a platform-independent program and achieved nearly perfect scalability on various massively parallel processing (MPP) systems (e.g., about 350 speedup on a 512-node Cray-T3E computers).

Rosenbluth and Hinton [7] emphasized the importance of an accurate prediction of the undamped component of turbulence-generated poloidal flows in determining the transport level in nonlinear turbulence simulations and provide an analytical test for predicting the residual flow level in response to an initial flow perturbation. We reproduced this test in gyrokinetic particle simulations by solving the collisionless toroidal gyrokinetic equation with an initial source that is constant on a flux surface and introduced a perturbation of the poloidal flow. This flow was relaxed through the transit time magnetic pumping effect, followed by a slower damped oscillation with a characteristic frequency corresponding to that of the geodesic acoustic mode (GAM). The residual level of this flow measured from the simulation agrees well with the theoretical prediction. In the nonlinear simulations of toroidal ITG instabilities, the $\mathbf{E} \times \mathbf{B}$ flows can be generated nonlinearly by the Reynolds stress [8]. Our global simulations clearly demonstrate the existence and the importance of such self-generated flows, in qualitative agreement with flux-tube simulations [9,10]. These simulations used representative parameters [2] of DIII-D $H$-mode core plasmas. The size of the plasma column was $a = 160\rho_i$. The simplified physics model includes the electron response of $\delta n_e/n_0 = e(\Phi - \langle\Phi\rangle)/T_e$, where $\langle\cdots\rangle$ represents the flux surface average. In a typical nonlinear simulation, we calculated 5000 time steps of the trajectories of 100 million guiding centers interacting with the self-consistent turbulent field, which was discretized by 25 million (128x768x256) grid points in a 3-dimensional configuration. The instabilities

evolved from a linear phase of growth to nonlinear saturation with a peak transport level, and finally to fully developed turbulence with a steady state transport level that is insensitive to initial conditions. To illustrate the effects of these flows on transport, we also carried out simulations of the same set of parameters with $\mathbf{E} \times \mathbf{B}$ flows suppressed by forcing $\langle \Phi \rangle = 0$. Comparison of the time history of $\chi_i$ from the simulation with turbulence-driven $\mathbf{E} \times \mathbf{B}$ flows included to that from the simulation with the flows suppressed shows that a significant reduction (up to an order of magnitude) in the steady state ion heat conductivity occurs when $\mathbf{E} \times \mathbf{B}$ flows are retained.

A key mechanism for reducing transport by $\mathbf{E} \times \mathbf{B}$ flows is the breaking of turbulent eddies and, consequently, the reduction of the radial correlation length [11,12]. This effect is visualized in a comparison of the poloidal contour plots of the fluctuation potential in the nonlinear phase from a broad pressure profile simulation carried out with $\mathbf{E} \times \mathbf{B}$ flows included to one with the flows suppressed (Fig. 1). In both cases, the amplitude of fluctuations is highest at larger major radius where the drive of instabilities is strongest due to a bad magnetic curvature. Similar structures are observed in the linear phase for both cases. $\mathbf{E} \times \mathbf{B}$ flows, which are linearly stable, are generated in the nonlinear saturation stage through inverse cascade of spectrum [13] and begin to tear apart the turbulent eddies. In steady state, the fluctuations are observed to be nearly isotropic in the radial and poloidal directions when $\mathbf{E} \times \mathbf{B}$ flows are included in the simulations, whereas the turbulent eddies are elongated along the radial direction when the flows are suppressed. The fact that the breaking of turbulent eddies by $\mathbf{E} \times \mathbf{B}$ flows results predominantly in the reduction of the radial correlation length is also reflected in the observed flow-induced broadening of the radial spectrum ($k_r$) of fluctuations [3]. These trends are in qualitative agreement with theoretical predictions [11,12]. We also observed that this flow-induced broadening of the $k_r$ spectrum is accompanied by a reduction in fluctuation level, although we have not studied the relation between them in detail. Finally, the $\mathbf{E} \times \mathbf{B}$ flows also broaden the frequencies spectrum of individual modes, which would otherwise possess a coherent mode history corresponding to a frequency spectrum with a well-defined peak.

Fluctuating flows with a radial characteristic length comparable to that of the ambient turbulence have been generated in flux-tube simulations [9,10]. On the other hand, $\mathbf{E} \times \mathbf{B}$ flows with scale lengths on the order of the system size have been the dominant feature in previous global gyrokinetic simulations although the finer scale flows began to appear in a larger system size [14]. These fundamentally different trends have been attributed to differences between global and local simulation models. Specifically, the whole plasma volume is simulated in global codes with pressure gradient profile variation and fixed boundary conditions, whereas local codes have a simulation domain that covers a few turbulent decorrelation lengths with a uniform pressure gradient and usually utilize radially periodic boundary conditions. We carried out simulations using both global and annular geometry with a variety of boundary conditions to address these differences. The perturbed electrostatic potential was set to zero at the boundary in all global simulations, and a radially periodic boundary condition was implemented in the annulus simulations. The profile of the pressure gradient was varied in the global simulations to distinguish the effects of profile variations from that of boundary conditions. When the profile of the pressure gradient was broad in the global simulations, the dominant components of the $\mathbf{E} \times \mathbf{B}$ flows have radial characteristic scale lengths comparable to the turbulence decorrelation length and characteristic frequencies comparable to those of the turbulence. Similar structures for the $\mathbf{E} \times \mathbf{B}$ shearing rate and good agreement in the ion heat conductivities were obtained between the local and global simulations (within 20%). These results indicate that the periodic boundary conditions in local codes are not responsible for the differences between the trends observed in local and global simulations. As the variation in the pressure gradient becomes stronger in the global simulation, a static single-well structure in the radial electric field, similar to those observed in previous global codes [14], emerges and becomes dominant. The ion heat conductivities also decrease because of the profile variation effects. We conclude that the narrow pressure gradient profile in global codes is responsible for the differences with the local code results.

## III. SHEARING RATE OF TIME-DEPENDENT E × B FLOW

To address the reduction of turbulence in the presence of zonal flows, we consider a model problem in which the potential $\Phi$ associated with the zonal flows is a time-dependent flux function, $\Phi(\psi,t) = \Phi_0(\psi)exp[-i\omega_f(t-t_0)]$, with the corresponding radial shear of the angular frequency, $\Omega_\psi \equiv -\partial^2\Phi_0(\psi)/\partial^2\psi$. The two-point correlation evolution equation is then derived following the procedure described in Ref. [3]. Results show that the radial correlation length $\Delta r$ is reduced by the flow shear relative to its value $\Delta r_0$ determined by ambient turbulence alone: $(\Delta r_0/\Delta r)^2 = 1 + \omega_{\rm Eff}^2/\Delta\omega_T^2$, where $\Delta\omega_T$ is the decorrelation rate of ambient turbulence and

$$\omega_{\rm Eff} \equiv \omega_E^{(0)} \frac{[(1+3F)^2+4F^3]^{1/4}}{(1+F)\sqrt{(1+4F)}}$$

is the effective shearing rate. Here, $F \equiv \omega_f^2/\Delta\omega_T^2$, and $\omega_E^{(0)} \equiv \Omega_\psi R B_\theta \Delta r_0/\Delta\phi$ is the instantaneous shearing rate, $R\Delta\phi$ is the toroidal correlation length. We expect that an order unity reduction of the fluctuations occurs if $\omega_{\rm Eff} \geq \Delta\omega_T$. When $E_r$ varies slowly such that $F \ll 1$, we have $\omega_{\rm Eff} \sim \omega_E^{(0)}$, and recover the previous result in general toroidal geometry [10]. When $E_r$ varies rapidly such that $F \gg 1$, we have $\omega_{\rm Eff} \ll \omega_E^{(0)}$, and it is difficult to achieve turbulence suppression. This is because the flow pattern changes before eddies get distorted enough. This provides an explanation of our gyrokinetic simulation results [2] which show a considerable reduction, but not complete suppression of turbulent transport although the instantaneous $\mathbf{E}\times\mathbf{B}$ shearing rate, part of which varies roughly on the turbulence time scale, is much larger than the maximum linear growth rate.

## IV. LINEAR MICROINSTABILITY ROTATION MODELS

We have developed a more complete rotation model in the FULL [4] comprehensive linear microinstability code to assess the effect of $\mathbf{E}\times\mathbf{B}$ flows on the high-$n$ toroidal drift modes destabilized by the combined effects of ion temperature gradients and trapped particles. This model allows general flux-coordinate toroidal geometry and includes contributions to

the radial electric field from toroidal and poloidal rotations and from the ion pressure gradient. Application to TFTR enhanced reversed shear (ERS) cases confirms the well-known heuristic criterion for complete stabilization, *i.e.*, that the $\mathbf{E} \times \mathbf{B}$ rotation shearing rate be greater than the linear growth rate without rotation. The implementation of this new ($E_r$) rotation model with the ballooning representation was described in some detail in Ref. [4]. A prescription for the ballooning parameter $\theta_0$ is needed, in addition to the rotation model itself. The simplest choice, $\theta_0 = 0$, which is the usual choice in the absence of rotation, was employed in Ref. [3]. However, a better prescription can be determined as follows: One-dimensional (ballooning representation) and two-dimensional calculations for toroidal drift modes have been compared for the old rotation model in Ref. [15], and a way of modeling one of the missing two-dimensional effects, 'eigenfunction shearing', in the one-dimensional calculation was found there by modeling the 'average' or 'effective' value of $\theta_0$ as a fitted function of the local Mach number. This additional 'eigenfunction shearing effect' decreases the maximum growth rate only moderately, and the radial marginal points where $\gamma = 0$ are barely moved. We conclude that including the two-dimensional 'eigenfunction shearing' effect in the ballooning representation calculation changes the results only moderately.

## V. RECENT DEVELOPMENTS IN GYROKINETIC THEORY AND SIMULATION

A gyrokinetic system for arbitrary wavelength perturbations is derived using the phase space Lagrangian Lie perturbation method which allows us to treat the background inhomogeneity and kinetic effects rigorously [16]. We have applied this self-consistent, comprehensive, and fully kinetic approach to study MHD instabilities and electromagnetic drift waves. By decoupling the gyromotion from the particle's gyrocenter orbit motion instead of averaging out the gyromotion, we have derived a gyrokinetic equation to describe the gyrokinetic perpendicular dynamics. This complete treatment of the perpendicular current enables us to recover the compressional Alfvén wave and arbitrary frequency modes such as

Bernstein waves from the gyrokinetic model.

We have devised an efficient and less noisy "split-weight" $\delta f$ scheme for treating electron dynamics in gyrokinetic simulation [17]. Each electron's response to the perturbations is split into an adiabatic and a nonadiabatic part. Evolution of the nonadiabatic part is dynamically followed and is determined by means of the continuity equation for perturbed charge density and current. This scheme has been validated for microinstability simulation in slab geometry.

The theory and implementation of the $\delta f$ method for plasma simulation are revisited [18]. Statistical coarse-graining techniques are used to give a rigorous derivation of the equation for the fluctuation $\delta f$ in the particle distribution. It is shown that for dynamically collisionless situations a generalized thermostat or "$w$-stat" may be used in lieu of a full collision operator to absorb the flow of entropy to unresolved fine scales in velocity space and saturate the system.

## VI. CONCLUSIONS

Massively parallel global gyrokinetic particle simulations have demonstrated decorrelation of nonlinearly saturated turbulence, and reduction of associated transport by self-generated zonal flows. Effective shearing rate of these time-dependent $\mathbf{E} \times \mathbf{B}$ flows has been analytically derived. Finally, linear microinstability calculations with an improved rotation model has been applied to experimental data.

Work supported by DoE Contract No. DE-AC02-76CH03073 and in part by the Numerical Tokamak Turbulence Project.

## FIGURES

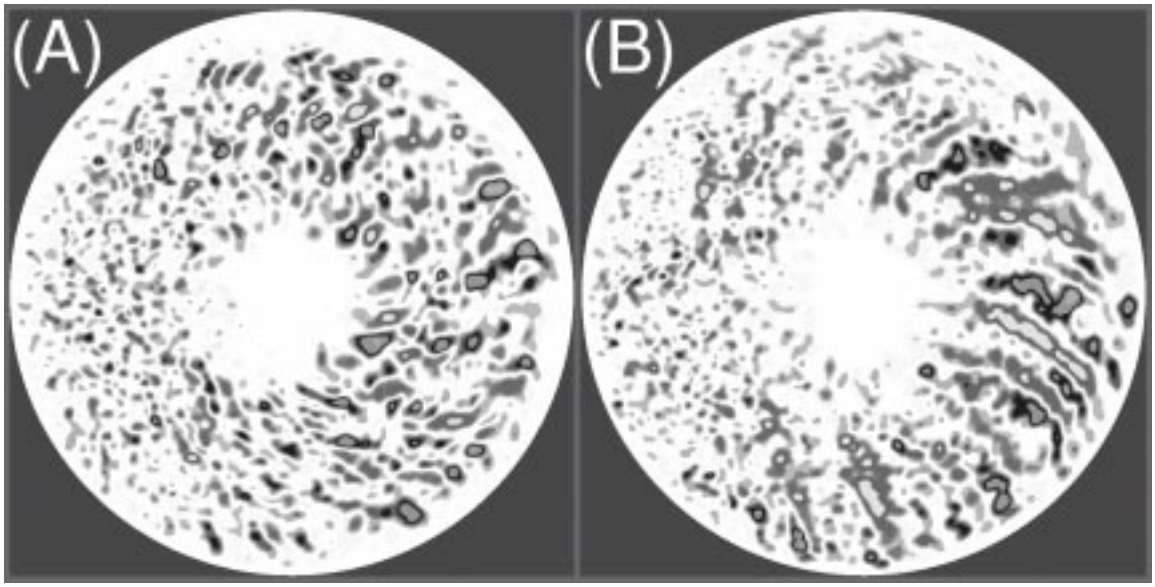


FIG. 1. Poloidal contour plots of fluctuation potential ($e\Phi/T_i$) in the steady state of a nonlinear global simulation with $\mathbf{E}\times\mathbf{B}$ flows included (A) and with the flows suppressed (B).

## REFERENCES


[1] R. Bell *et al.*, *Phys. Rev. Lett.* **81**, 1429 (1998).

[2] Z. Lin, T. S. Hahm, W. W. Lee, W. M. Tang, R. B. White, *Science* **281**, 1835 (1998).

[3] T. S. Hahm *et al.*, *Phys. Plasmas* **6**, 922 (1999).

[4] G. Rewoldt *et al.*, *Phys. Plasmas* **5**, 1815 (1998).

[5] Z. Lin, W. M. Tang, W. W. Lee, *Phys. Rev. Lett.* **78**, 456 (1997).

[6] Z. Lin and W. W. Lee, *Phys. Rev.* E **52**, 5646 (1995).

[7] M. N. Rosenbluth and F. L. Hinton, *Phys. Rev. Lett.* **80**, 724 (1998).

[8] P. H. Diamond and Y. B. Kim, *Phys. Fluids* B **3**, 1626 (1991).

[9] G. W. Hammett, *et al.*, *Plasma Phys. Contr. Fusion* **35**, 973 (1993).

[10] A. M. Dimits *et al.*, *Phys. Rev. Lett.* **77**, 71 (1996).

[11] H. Biglari, P. H. Diamond, P. W. Terry, *Phys. Fluids* B **2**, 1 (1990).

[12] T. S. Hahm and K. H. Burrell, *Phys. Plasmas* **2**, 1648 (1995).

[13] A. Hasegawa and M. Wakatani, *Phys. Rev. Lett.* **59**, 1581 (1987).

[14] R. D. Sydora *et al.*, *Plasma Phys. Control. Fusion* **38**, A281 (1996).

[15] G. Rewoldt *et al.*, *Phys. Plasmas* **4**, 3293 (1997).

[16] H. Qin *et al. Phys. Plasmas* **5**, 1035 (1998).

[17] I. Manuilskiy *et al.*, *Bull. Am. Phy. Soc.* **43**, 1723 (1998)

[18] J. A. Krommes, *Bull. Am. Phy. Soc.* **42,** 1982 (1997)